Sampling Interplanetary Dust from Antarctic Air

S. Taylor[1*], J. H. Lever[1], R. M. Stroud[2], K. D. Burgess[2], D. E. Brownlee[3], L. R. Nittler[4], A. Bardyn[4], C. M. O'D. Alexander[4], K.A. Farley[5], J. Treffkorn[5], S. Messenger[6^], and P. Wozniakiewicz[7].

[1]CRREL, 72 Lyme Road, Hanover NH 03755; [2]Materials Science and Technology Division, Naval Research Laboratory Washington, DC 20375; [3]Dept. of Astronomy, University of Washington, Seattle WA 91195; [4] Carnegie Institution of Washington, 5241 Broad Branch Rd NW, Washington DC, 20015; [5]Caltech, 1200 E California Blvd, Pasadena, CA 91125; [6]NASA Johnson Space Center, ARES, Code SR Houston, TX 77058; [7] School of Physical Sciences, University of Kent, Canterbury, CT2 7NH, UK. *retired, ^ self-employed.

Abstract

We built a collector to filter interplanetary dust particles (IDPs) larger than 5μm from the clean air at South Pole station. Our sampling strategy used long-duration, continuous dry filtering of near-surface air in place of short-duration, high-speed impact collection on flags flown in the stratosphere. We filtered ~10^7 m^3 of clean Antarctic air through 20-cm-dia, 3-μm filters coupled to a suction blower of modest power consumption (5 – 6 kW). Our collector ran continuously for two years and yielded 41 filter samples for analyses. Based on stratospheric concentrations, we estimated that each month's collection would provide 300 – 900 IDPs for analysis.

We identified 19 extraterrestrial (ET) particles on the 66 cm^2 of filter examined, which represented ~ 0.5% of the exposed filter surfaces. This number of ET particles is about a third of the expected value. Of the 19 ET particles identified, four were chondritic porous IDPs, seven were FeNiS beads, two were FeNi grains and six were chondritic material with FeNiS components. Most were <10μm in diameter and none were cluster particles. Additionally, a carbon-rich candidate particle was found to have a small ^{15}N isotopic enrichment, supporting an extraterrestrial origin. Many other candidate grains, including chondritic glasses and C-rich particles with Mg and Si and FeS grains, require further analysis. The vast majority of exposed filter surfaces remain to be examined. Filters are now curated at Johnson Space Center in Houston, and will soon be available for request from Astro materials Research and Exploration Science division.

Introduction

Extraterrestrial (ET) materials that are collected on Earth include interplanetary dust particles (IDPs) collected in the stratosphere and micrometeorites (MMs) collected at the Earth's surface (Taylor et al., 2016a). Among them, the chondritic porous anhydrous particles (CP-IDPs) are thought to originate from comets (Ishii et al., 2008). They are characterized by the presence of anhydrous crystalline phases, amorphous phases such as GEMS (glass with embedded metal and sulfides [Bradley, 1994]), high abundances of presolar grains (Busemann et al., 2009, Messenger et al. 2003), high organic C contents (Thomas et al., 1993) and H, C, and/or N isotopic anomalies in the organics (Messenger, 2000). Interestingly, both CP-IDPs and larger ultra-carbonaceous micrometeorites (UCAMMs), likely also of cometary origin, were recently collected by melting large volumes of Antarctic snow [Noguchi et al., 2015; Dobrica et al., 2009; Duprat et al., 2010; Dartois et al. 2013]. The presence of highly primitive ET materials in recent Antarctic snow indicates that they may also be collected directly from the air, thus allowing laboratory analysis of potentially cometary particles with minimal terrestrial alteration.

Since the 1970s, IDPs have been collected in the stratosphere with high flying aircraft. Brownlee et al. (1977) examined silicone-oil coated 'flags' (30 cm^2) exposed in the

stratosphere during 200 hours of U2 flights (~ 20 km altitude). They found 300 IDPs in the size range 8 – 60 μm from a swept volume of 2.5 x 10^5 m^3. This yields a particle concentration of 1.2 × 10^{-3} m^{-3} assuming 100% collection efficiency. Zolensky and Mackinnon (1985) analyzed particles larger than 1 μm from a similar collector plate and estimated an IDP concentration of 5 × 10^{-2} m^3 for 1 – 40 μm sized particles, with 5% or 2.5 × 10^{-3} m^{-3} being larger than 5 μm. To avoid using flags coated with silicone oil Messenger et al. (2015) collected IDPs using polyurethane foam on the stratospheric flags, but significant particle fragmentation occurred as a result of 200 m/s impact.

Direct filtering of air has advantages over stratospheric capture or terrestrial melting and filtering snow and ice. These include low stress on the particles, no contamination by oil and solvents, minimizing contact with water, a continuous record of IDP fluxes and characteristics, and lower costs. Air filtering was first tried at the South Pole using an electrostatic precipitation particle collector (Witkowski, 1988). The experiment ran for over 2 years, and although many particles were collected only one had chondritic elemental ratios. Identifiable contaminants included sulfuric acid droplets and sooty carbonaceous material. Wozniakiewicz et al. (2014) filtered air from the island of Kwajalein in the Republic of the Marshall Islands by means of commercial air sampler that pulled 8 ×10^{-3} m^3/s of air up through a rain hood and down through a 20-cm × 25-cm, 5-μm polycarbonate filter. The filters were washed to remove salt encrustations and concentrate particles, some of which had morphologies or compositions consistent with micrometeorites. Similar equipment is being used to sample air atop Mauna Loa, Hawaii (Ishii et al. 2018) and at the Halley research station in Antarctica (Alesbrook et al. 2017).

The South Pole has many advantages for this type of collection. Lack of upwind human activity, depression of the tropopause, general lack of deep atmospheric convection, and high altitude (2835m) greatly diminishes the flux of terrestrial contaminants in the air. NOAA operates Atmospheric Research Observatory (ARO) at South Pole as a clean air reference station. The air is the cleanest on Earth and has the fewest aerosols (Hogan et al. 1979). The austral summer aerosols are primarily sulfuric acid droplets, 0.03-0.005 μm in diameter (Ito 1985) whose numbers (~300/cm^3) decrease by an order of magnitude during the austral winter relative to their summer peak (Bodraine and Murphy 1980). During the austral winter, sea salt and ammonium sulphate particles are the primary aerosol (Ito 1985) that arrive at the Pole when storms off the Antarctic coast advect ocean air into the continent. Less than 2% of the aerosols derive from the terrestrial crust (Hogan et al. 1979). The main disadvantage of sampling at South Pole is its relative inaccessibility. Any shipping, constructing, testing or modifying associated with the collector has to occur during the four-month summer season. Additionally, samples are also returned during this four-month window providing little time for the analyses needed to refine collecting procedures before the station closes for the winter.

We built and operated a collector with an order-of-magnitude higher flow rate than commercial equipment to filter IDPs larger than 5μm from ultra-clean air at the Amundsen Scott South Pole station (Taylor et al. 2016b). Based on stratospheric concentrations we estimated that each month's collection would provide 300 – 900 IDPs for analysis. Such a large, clean, and time-stamped collection would make it possible to: (1) characterize the meteoroid complex throughout the year; (2) identify episodic or periodic events such as meteor streams; (3) collect rare, large cluster particles (>30μm) that have short atmospheric-residence times (< 1 day) and thus can be associated with specific events such as fireballs or meteor-stream crossings. Here, we describe our experimental design and the results obtained on ET particles from 15 filters

examined and ^{3}He measurements from 13 filters analyzed of the 41 filters collected during the two-year test.

Materials and Methods

The collector

In 2016, we designed, built, tested and installed a collector to suction interplanetary dust particles (IDPs) from the clean-air sector at South Pole station. Important design considerations were that it be simple, suction air at approximately the average wind speed at South Pole (5 – 6 m/s), work at cold temperatures, and allow for easy filter exchanges while keeping the filters clean. We anticipated monthly manual filter changes, with the option of more frequent changes if desired.

Winds at South Pole entrain essentially all IDPs of interest. IDPs have decelerated to their settling velocities by the time they reach stratospheric altitudes, and they slow about 10% more at near-surface air viscosities. Assuming Stokes flow, IDP settling velocities for spherical particles range from about 10^{-3} m/s for a 5 μm particle of density 1 g/cm^3, to 0.3 m/s for a 50 μm particle of density 3 g/cm^3 (Flynn and Sutton, 1991). Irregularly shaped IDPs should settle more slowly. Consequently, we oriented our collector pipe horizontally to ingest the wind-entrained IDPs. Somewhat arbitrarily we selected a target of 300 IDPs larger than 5 μm collected for each monthly filter exposure. At an intake speed of 5 m/s through a 3-μm filter, this target set the filter diameter at 20 cm and the suction-blower power requirement at 5 kW. We thus expected to collect about one IDP per cm^2 of filter area per month of exposure, equivalent to 50 – 200 hours of stratospheric flights.

The collector was in a dedicated building placed on a raised snow berm located on the border of the clean air sector (Fig. 1A). The air intake pipe was 8 m above the snow surface to minimize ingesting blowing snow that travels near the snow surface (Mellor, 1965). Air was drawn in through a 20 cm diameter aluminum pipe and then a 20 cm diameter filter unit (Fig. 1B). The filter unit consisted of a polycarbonate membrane (3-μm pores at a density of 2×10^6 pores/cm^2) clamped between two aluminum rings held together with cable ties (Fig. 1C). The filter unit was assembled in a clean room and then shipped to South Pole where it was inserted and clamped in the collector (Fig. 1D). We selected aluminum for the collector components (6061 T-6) as Al is easy to recognize as a contaminant compared to stainless steel or mixed metals, and it is more durable than most plastics at the low temperatures and high wind speeds possible at South Pole. Power was obtained via a buried electrical cable from the Atmospheric Research Observatory (ARO). Our NSF assigned research associate made weekly measurements on the blower current draw, flow rate, pressure drop across the filter and the temperatures entering and exiting the collector (Appendix A). Most importantly, the associate changed the filters during the year, nominally at monthly intervals.

Daily weather summaries showed generally steady winds ~5 m/s, from the northeast quadrant (clean sector). During the two years of the project, winds were from the clean air sector 92% of the time, intermediate to published values, 89% (Sheridan et al. 2016) and 98% (Bodhain et al. 1986). NOAA noted clean air sector violations (Appendix A), generally local, short-term occurrences (e.g. snow mobile deliveries to ARO) that could nevertheless impact our samples.

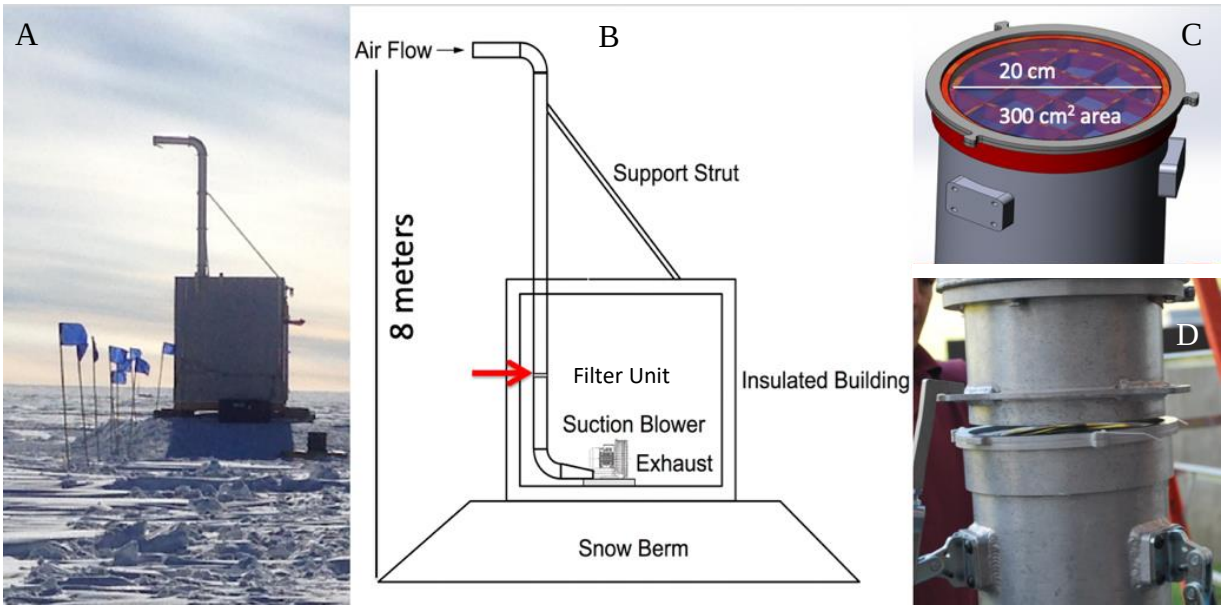

Fig. 1. A) Photo of building housing our experiment. B) Schematic of the collector, arrow shows the location of the filter unit. C) Schematic of filter unit. D) Image of filter unit and toggles used to secure it in pipe.

Sample preparation and ET Searching Techniques

Our group used a variety of approaches to search for ET particles. Using a light microscope, we searched small areas of filters SPA-4, 5, 12 for rare, >30µm cluster particles. A total of 70 particles were manually removed and examined with an SEM. We also used SEMs to examine sections of filters (SPA-3, 4, 10, 11, 14, 17 and 22) mounted on Al stubs or on microscope slides. The filter pieces were cut using stainless steel scissors and attached to double-sided carbon or copper tape before coating with carbon, <30 nm thickness, or iridium (SPA-4 and 11). Mg and Fe element maps were made of the iridium coated samples (200 µm by 300 µm frames) to identify candidate ET particles. Lastly, we removed particles from cm^2 filter sections by pressing a carbon sticky mat against the filter (SPA-1, 4, 10, 17, 35, 39). Generally, the carbon mat was pressed once onto the filter but in the case of SPA-5 we also made a 0.5 cm^2 'stamp' used to lift particles from a ~4 cm^2 section of the filter.

We targeted high Z (bright) grains, fluffy (multiple components) particles, spheres, and low Z (dark) grains composed mainly of C with some chondritic signature or with high N concentrations. Multiple components particles with intricate structure are characteristics not shared by most contaminants. Particles were determined to be ET if their spectra showed the presence of Fe, Ni, Mg, Si, and S in chondritic proportions. Candidate ET particles were identified by qualitative comparison to bulk chondritic composition, presence of N and, or Ni, or as pure Mg-silicate grains (very low Fe). We took images of all particles that were ET and also imaged common contaminants found on each filter. The filters were stored in the bags and Al holders in which they were received, and every effort was made to avoid contamination by dust in the lab.

Electron Beam Analytical Methods

Scanning Electron Microscopy (SEM): S.T. (with students Amanda Pinson and Summer Christenson) used a FEI Scios 2 SEM located at Dartmouth College. The secondary electron detector highlighted topography while the backscatter electron detector highlighted composition (atomic number). An energy-dispersive X-ray (EDAX) spectrometer provided quantitative

compositional data. Imaging and EDS was mostly done at 20 kV.

R.S. and K. B. (with student intern David Bour) used a FEI Helios G3 FIB-SEM and FEI Nova 600 FIB-SEM at the Naval Research Laboratory (NRL) to search for particles. A secondary electron image with FOV 518 or 638 μm, provided a large search area while seeing particles >~3 μm (size of filter holes). Each particle within this FOV was measured using EDS spot analysis for "bulk" composition. Imaging and EDS was mostly done at 15 kV in order to include Fe-Kα, but some measurements were done at 5 kV, which shows surface structure of the particles with more detail.

A. B., C.A., and L. N. used a JEOL 6500F SEM at the Carnegie Institution of Washington (CIW). About 1 cm^2 of filter was cut, placed on a C sticky tab and coated with Ir. SEM and EDS maps were acquired at 15 kV with a frame size of 200 μm × 300 μm. Candidate ET grains were identified as hotspots in Mg and Fe EDS maps and reanalyzed at high magnification.

TEM sample preparation: K.B. used a FEI Helios G3 at NRL for Focused Ion Beam (FIB) sample preparation of a few candidate ET grains. After deposition of a protective carbon strap, samples were milled using a 30 kV Ga^+ beam, and final thinning for most samples was done at lower voltage, 5 kV. K. B. also embedded one particle in sulfur and used an ultramicrotome equipped with a diamond knife to section it for analysis by both NanoSIMS and STEM. Samples for NanoSIMS were cut to a thickness of 150 nm and mounted on a silicon wafer, while samples for STEM were 70 nm thick and mounted on 200 mesh Cu TEM grids with a carbon support film. The sulfur was removed by sublimation in a 60 °C oven for at least 2 h.

Scanning Transmission Electron Microscopy (STEM): K.B. used the Nion UltraSTEM200-X at NRL for STEM analyses. The microscope is equipped with a Gatan Enfinium ER spectrometer for electron energy loss spectroscopy (EELS) and a windowless, 0.7 sr Bruker SDD detector for energy dispersive spectroscopy (EDS). The STEM was operated at 60 kV for carbon-rich samples and 200 kV for silicate and sulfide samples. Images were collected using bright field (BF) and high-angle annular dark field (HAADF) modes.

Nano Secondary Ion Mass Spectroscopy (NanoSIMS): L. N. and A. B. used the Cameca NanoSIMS 50L ion microprobe at CIW to measure Mg-Al isotopes in one ET particle mounted on C sticky tape and H, C, and N isotopes in microtomed slices of a C-rich candidate ET particle. For the Mg-Al measurements a ~100-nm, ~4pA O^- primary beam was rastered (256×256 pixels, 8 μm) over the sample with simultaneous collection of ^{23}Na, $^{24,25,26}Mg$, ^{27}Al, ^{28}Si, and ^{56}Fe positive secondary ions in multicollection mode. For the H, C, and N measurements, a focused Cs^+ primary ion beam was used, again in multicollection imaging mode (256×256 pixels, 20-22 μm). A ~4 pA beam was used for the H measurements, with collection of $^1H^-$, $^2H^-$, $^{12}CH^-$ and $^{18}O^-$ ions, whereas for C and N, a ~1 pA beam was used and $^{12}C_2^-$, $^{12}C^{13}C^-$, $^{12}C^{14}N^-$, $^{12}C^{15}N^-$, and $^{28}Si^-$ secondary ions were measured. Images were analyzed with the L'image software (L. Nittler, CIW) following essentially the same methods described by Nittler et al. (2018). A synthetic organic powder with known isotopic composition was used as an isotope standard for the H measurements. For C and N, insoluble organic matter extracted from a CR chondrite meteorite and microtomed slices of superglue were used as standards.

Helium-3 measurements

Helium-3 is a stable non-radiogenic isotope that is in quite high concentration in IDPs but not in terrestrial samples. The high concentrations arise from the implantation of solar wind ions on or near IDP surfaces while the IDPs are in space. As solar wind $^3He/^4He$ ratios are far higher than terrestrial ones, ^3He can be used as an ET tracer. Helium-3 measurements were made on 13 of the filters to determine if they contained ET material, to look for a seasonal variation in the ET flux and to check if the airflow was even across the filter. We also used glass filters to wipe the insides of the intake pipes at the end of the experiment to check for adhering ET material.

K.F. and J.T. made ^3He measurements on 180, 1-cm^2 subsamples cut from 13 of the filters. Also, 10 Whatman glass filters (47 mm in diameter) were used to wipe the insides of the intake pipes. S.T. placed each 1-cm^2 polycarbonate filter subsample or glass filter in a tin foil cup and compressed it to form a compact ball. These samples were sent to Caltech and measured with a Thermo Helix SFT mass spectrometer following the procedures used for ^3He extraction from seafloor sediments (Patterson and Farley, 1998). Unique to these analyses was a decontamination step to protect the vacuum purification line from organic contamination after the polycarbonate filters were analyzed (Farley et al, in prep).

Results

General

The collector ran well and continuously (except for short weather shut downs) from installation on 29 Nov. 2016 to project end on 6 Jan. 2019. The equipment survived -75 °C temperatures and 50 km hr^{-1} winds. During the two-year project, forty-one filters were exposed to the air stream for times ranging between 0.25 and 39 days (Fig. 2A). We exposed filters for different lengths of time to assess how aerosol loads affected ET numbers.

The blower sucked air through the filter at ~ 5m/s or about 400,000 m^3 a month (Appendix A). The pressure-drop measured across each filter showed that the filters did not plug significantly (Fig. 2B). The average pressure drop for a clean filter was 15.36 ± 1.1 kPa (Fig. 2B blue points), whereas it was 18.46 ± 1.8 kPa for an exposed filter (Fig. 2B red points). Although the data are noisy, the general trend was for pressure-drop to increase with increasing exposure time, as expected if particles or aerosols progressively plugged the filter pores. The average increase in pressure corresponded to about 25% of the pores being plugged during exposure and a decrease in flow rate of about 12%. The largest pressure-drop 23.25 kPa (3.37 psi) was measured before changing out filter SPA-35. Given the large volume of snow that accumulated on this filter (Fig. 2C), the pressure drop was surprisingly low and corresponded to a decrease in flow rate of only 22% compared with the average clean-filter value. Clearly, the snow that accumulated on the filters presented less flow restriction than the 3-μm filters themselves. If snow was present on the filters these were carefully removed to retain the snow and allow it to sublimate or melt in place.

Most of the filters appeared optically clean (Fig. 3A), but four were stained, three had a small hole or a rip (Fig. 3B), seven had dark particles on their surfaces and one was covered with carbon particles (Fig. 3C). The latter, SPA- 39, was not different from the other filters in terms of clean air violations or wind from non-clean air sectors (Appendix A). Even when optically clean, magnification revealed that ~10 μm Al metal from the intake pipe was a significant source of contamination on the filters. As Al particles from collector fabrication diminished with operating time, filters installed later in the experiment had fewer Al grains. Many of the Al grains were

easily distinguished from ET particles by their appearance (Fig. 4A), but some were dark and irregularly shaped like IDPs (Fig. 4B).

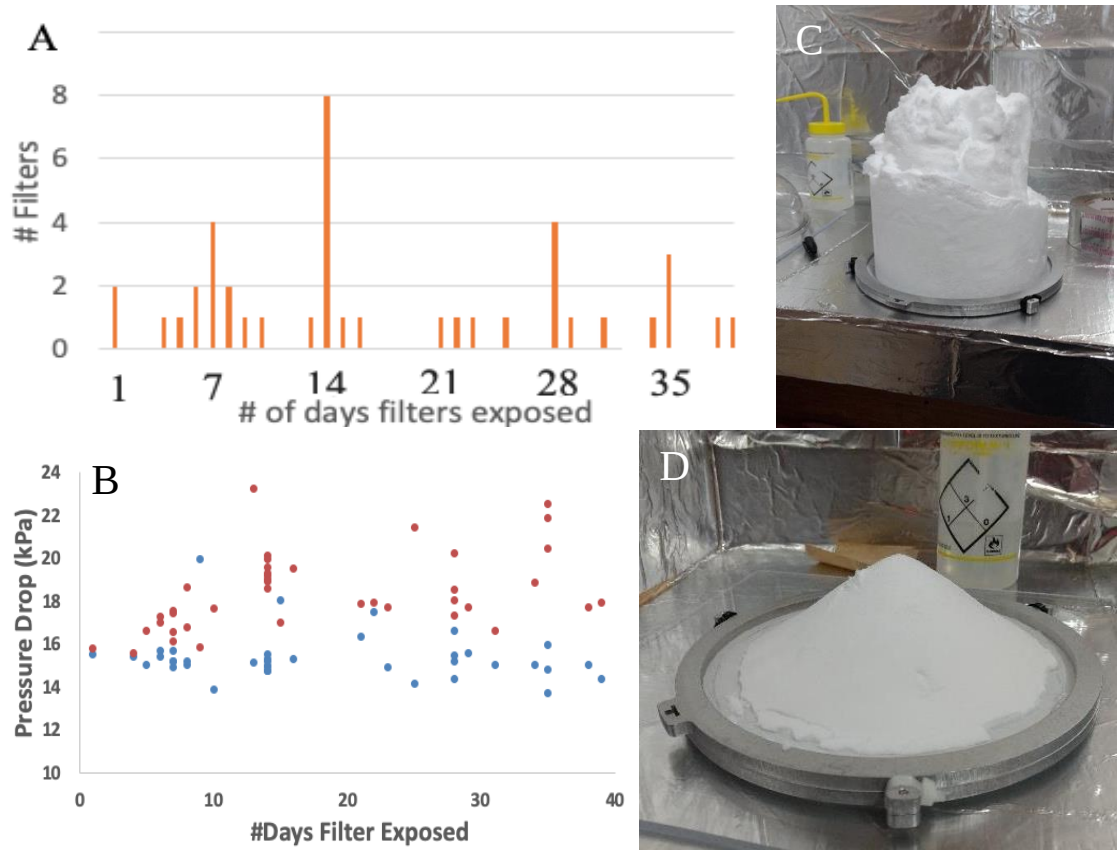

Fig. 2. A) Histogram of number of filters exposed for different number of days; B) Pressure drop across the filter (kPa) as a function of exposure time, (n=38) clean filters shown as blue dots, exposed filters shown as red dots; C) extreme, SPA-35, and D) normal, SPA-31, example of snow deposition on filters during storms.

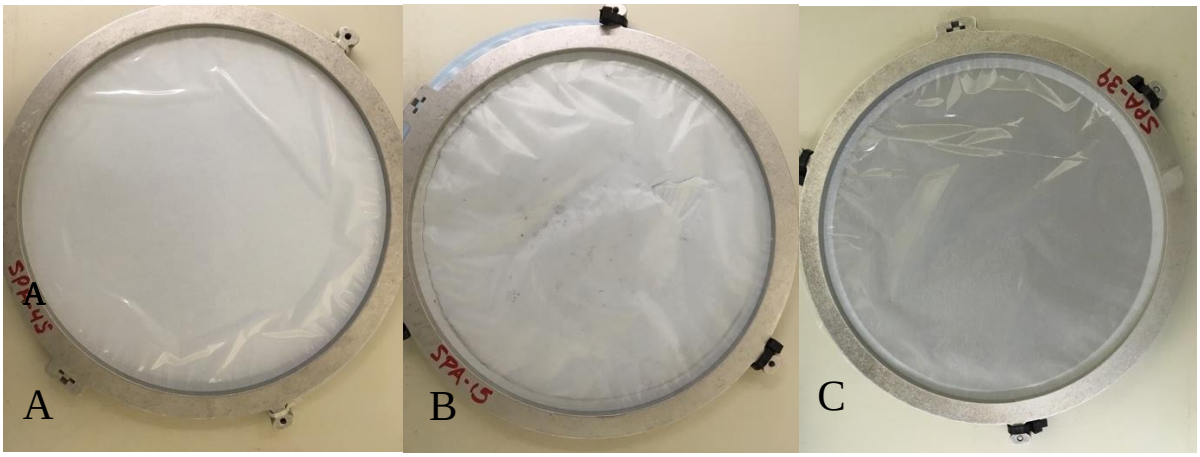

Fig. 3. Example of a clean (A), a dirty and ripped (B) and a singularly dirty (C) filter. The diameter of the filters is 20 cm in diameter resulting in a ~300cm^2 collecting area.

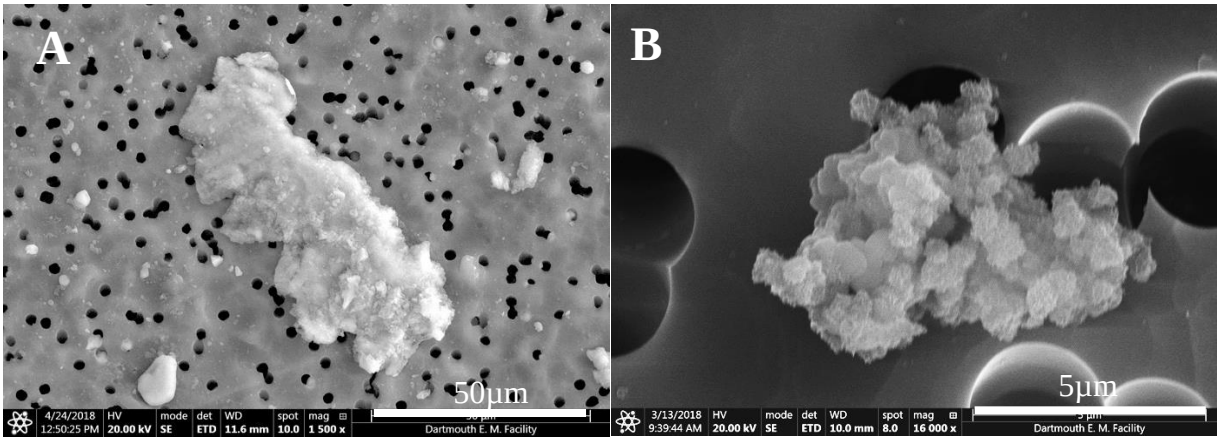

Fig. 4. A) Typical Al grains; B) Al grain that is morphologically similar to a fluffy IDP.

We expected most of the aerosols to follow the air stream through the pores, however, given the 400,000 m^3 of air we suctioned each month, some of the sulfuric acid droplets impinged on the filter surface (Fig. 5A), filled the pores (Fig. 5B), or decorated particle surfaces (Fig. 5C). The winter filters had fewer sulfuric acid droplets but many salt grains, some cubic in shape, some rods (Fig. 5D, E). The salt rods are common and often thin and delicate, suggesting that the collection process is gentle enough to not break them (Fig. 5D). The seasonal variation in aerosols noted here agrees with measurements made by others (e.g. Bodraine et al. 1986).

Other types of particles found include clay minerals, quartz grains, and the occasional diatom (Fig. 6A). We found no Al oxide spheres that were once common on stratospheric collection flags and thought to derive from rocket exhaust (Brownlee et al. 1976). The Fe-poor Mg-silicates we did find are likely talc contaminants from the weather balloons released at South Pole (Fig. 6B, C, D). Samples of this talc match the compositions of the Mg-silicates (Fig. 6C) and many talc particles are released when the balloons are inflated (Fig. 6D) and presumably when they are flown.

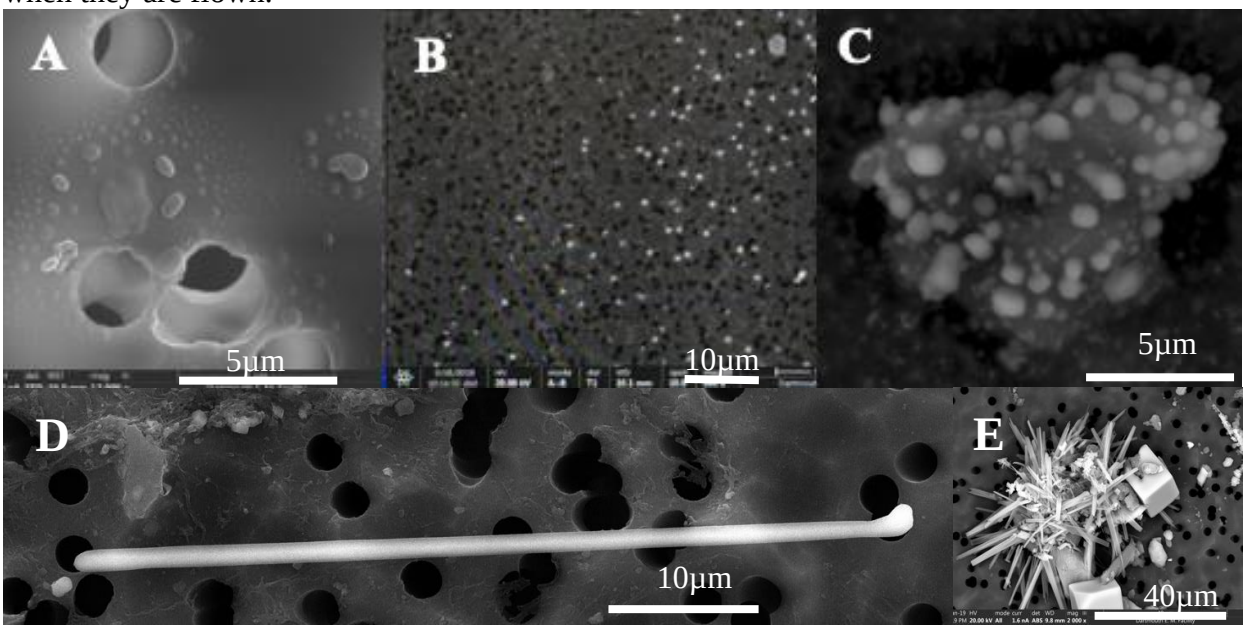

Fig. 5. Sulfuric acid droplets on a filter (A); infilling filter pores seen as bright circular features (B); and decorating an aluminum grain (C); Salt rod (D); Salt crystals and cubes (E).

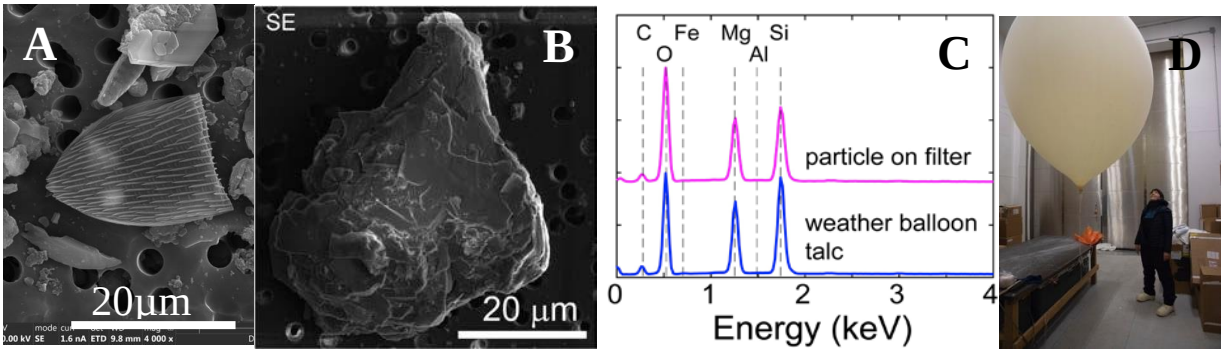

Fig. 6 A) Diatom; B) image of particle on filter; C) comparison of a particle on filter with weather balloon talc; D) inflation of weather balloon sheds many talc particles that appear as white powder on the table (Fig. 6D, R.S. for scale).

ET particles

Table 1 summarizes the ET particle search results. We examined ~ 66 cm^2 of filter from 15 different filters exposed to the Antarctic air over the course of two years. The average exposure for the filters containing the 19 ET particles was 32 days. We predicted one ET particle per cm^2 per month and found 0.3 ET particle per 32 days, or about a third of the ET particles expected. Of the 19 ET particles, four were chondritic porous IDPs (CP-IDPs), seven were FeNiS beads, two were FeNi grains, and six were chondritic material with FeNiS components. Most were <10µm in diameter, with an average diameter of 6±5 µm (n=19) compared with 11±6 µm measured for stratospheric ET particles (n=180) [Cosmic Dust Catalogs], and none were cluster particles. We found one particle that may be an ultra-carbonaceous ET particle and many other candidate grains that have chondritic glass compositions, which might be classified as cosmic in the stratospheric catalogs (Appendix B, C). We found only one olivine grain, a mineral which is ubiquitous in ET materials but also not common (2%) on the stratospheric collection flags imaged in the Cosmic Dust Catalogs we reviewed (Appendix C). In general, the appearance of the ET particles collected from the South Pole air are similar to those collected in the stratosphere. Below we describe a few of the ET particles in more detail.

SPA-1 was the first filter deployed and, although it was exposed for only 5 hours, the 1 cm^2 section examined contained an IDP (Fig.7a). The IDP had multiple phases, including a ~2-µm Fe-sulfide and smaller silicates, and a ~500-nm Al, Na-rich grain (likely a feldspar). We performed Al-Mg analysis of the IDP by NanoSIMS, but the Mg content of the Al-rich grain was too high to detect extinct ^{26}Al.

A FIB section cut through an Fe-sulfide grain and the STEM analysis of the section shows several 100-400 nm Fe-Ni metal inclusions (Fig. 7c). The edge of the grain, which was attached to the carbon tape substrate and thus protected from ion beam during preparation, shows a damaged rim, likely from exposure to the space environment (Fig. 7). Electron Energy Loss Spectroscopy (EELS) analyses show a hydrogen signature in the oxidized iron and in the vesicles found near the rim, possibly from alteration during atmospheric entry heating (Fig. 7d).

Table 1. Summary of information obtained from filters examined.

Season	Filter #	Days exposed	# ET	Ave. Diameter (µm)	Filter Area Examined (cm2)	Particles Analyzed	ET Particle Composition	Method Mounted	
Spr. 2016	SPA-1	0.25	1	5	1		CP-IDP	C sticky	Taylor
	SPA-3	5		40	1	238	UCAMM?	C coated filter	Stroud & Burgess
	SPA-4	35	1	5	2	53	FeNiS bead	coated filter	Alexander & Bardyn
			0		2				Taylor
Sum. 2017	SPA-5	25	2	11 & 15		50	FeNiS beads	50 picked	Brownlee
			0			20		20 picked	Brownlee
					4	15	chondritic glass	stamp	Taylor
Fall 2017	SPA-10	35	2	4 & 9	10.5	30	FeNiS, CP-IDP	C coated filter Z	Pinson & Taylor
			1	4	10	19	CP-IDP	C coated filter	Taylor
			1	9	1		CP-IDP	C sticky A	Taylor
			4	1,1,2, 3	1	7	3 beads, 1 bead+chon	C sticky B	Taylor
			1	5	1	4	1 chon+ FeNiS	C sticky C	Taylor
			1	5	1	3	1 chon+ FeNiS	C sticky D	Taylor
Win. 2017	SPA-12	15	0		1	8			Brownlee
	SPA-14	16	0		2.5	115			Stroud & Burgess
	SPA-15	39	0		1	5		coated filter	Taylor
Spr. 2017	SPA-17	22	0		9.7			C coated filter	Taylor
			1	10	1	25	FeNi	C sticky A	Taylor
	SPA-21	4	0		1	5		coated filter	Taylor
	SPA-22	14	0		10.8	24		C coated filter	Christensen & Taylor
Fall 2018	SPA-30	38	4	1,4, 5,15	1	12	3 Chon, 1 FeNi	coated filter	Taylor
Spr. 2018	SPA-35	13	0		1	10		coated filter	Taylor
	SPA-39	7	0		1	9		coated filter	Taylor
Sum. 2018	SPA-45	1	0		1	3		coated filter	Taylor
Total			**19**		**65.5**				

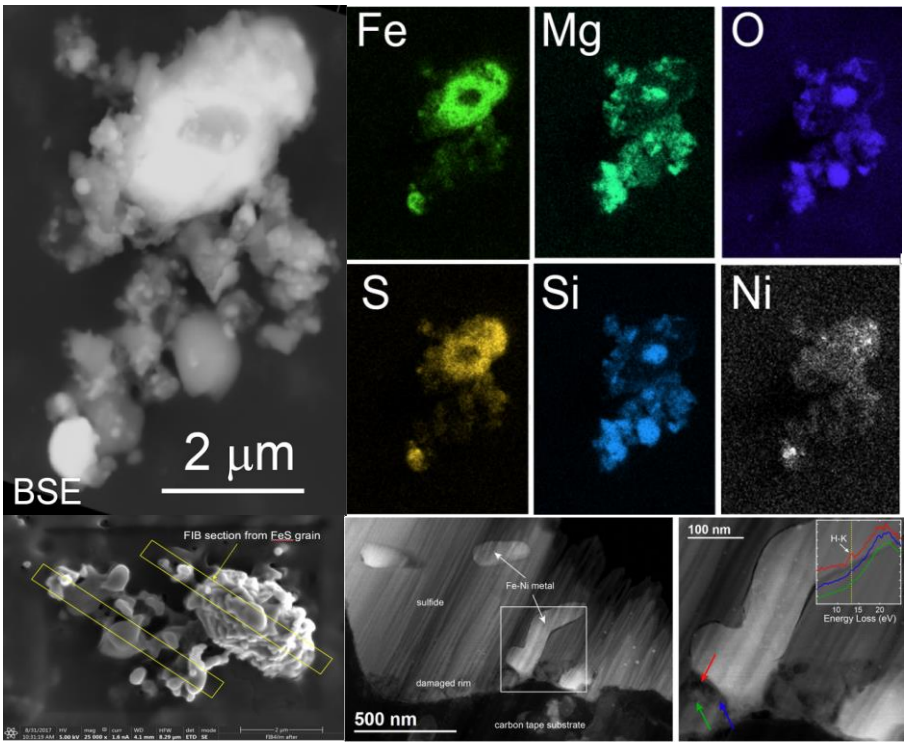

Fig. 7. Top, backscattered electron (BSE) image and select X-ray maps of the IDP from SPA-1 analyzed by NanoSIMS and STEM. Bottom, locations of FIB sections and a HAADF image of a FIB cross-section of sulfide grain with Fe-Ni metal inclusions and alteration rim. Inset shows the EELS data. The sub-vertical lines are artifacts of FIB preparation.

Fig. 8 illustrates the variety of ET particles found in ~ 24 cm^2 of filter SPA-10. The particles range from a submicron FeNiS bead (G) to a 15µm CP-IDP (I). Most contained FeNiS and many have chondritic material attached (B, C, D, E, G, I, and J). Below we describe additional analyses made on particles I and J.

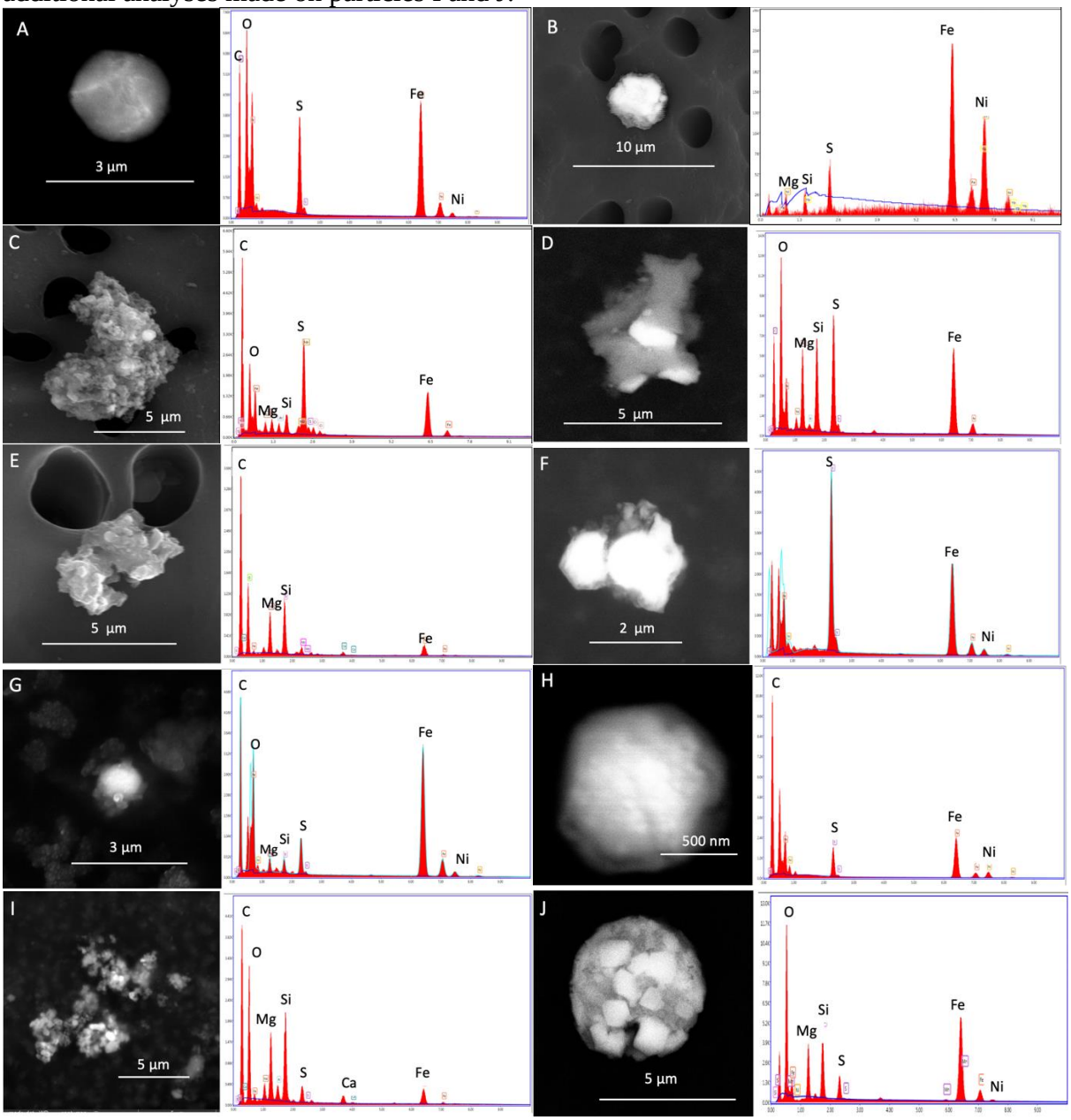

Fig. 8. Images and spectra of ten ET particles found on SPA-10. Two of these (I and J) have been analyzed in more detail and are discussed below.

Particle I is a CP-IDP of chondritic composition (Fig. 8-I). The FIB section (Fig. 9 A, B) shows crystals of enstatite and a high-Ca pyroxene (Fig. 9 C), olivine, Ni pyrrhotite, and magnetite (Fig. 9 D). Magnetite partial rims on some grains indicates atmospheric entry heating. Carbonaceous material is enclosed by one of these magnetite rims. Ni is present only in the pyrrhotite.

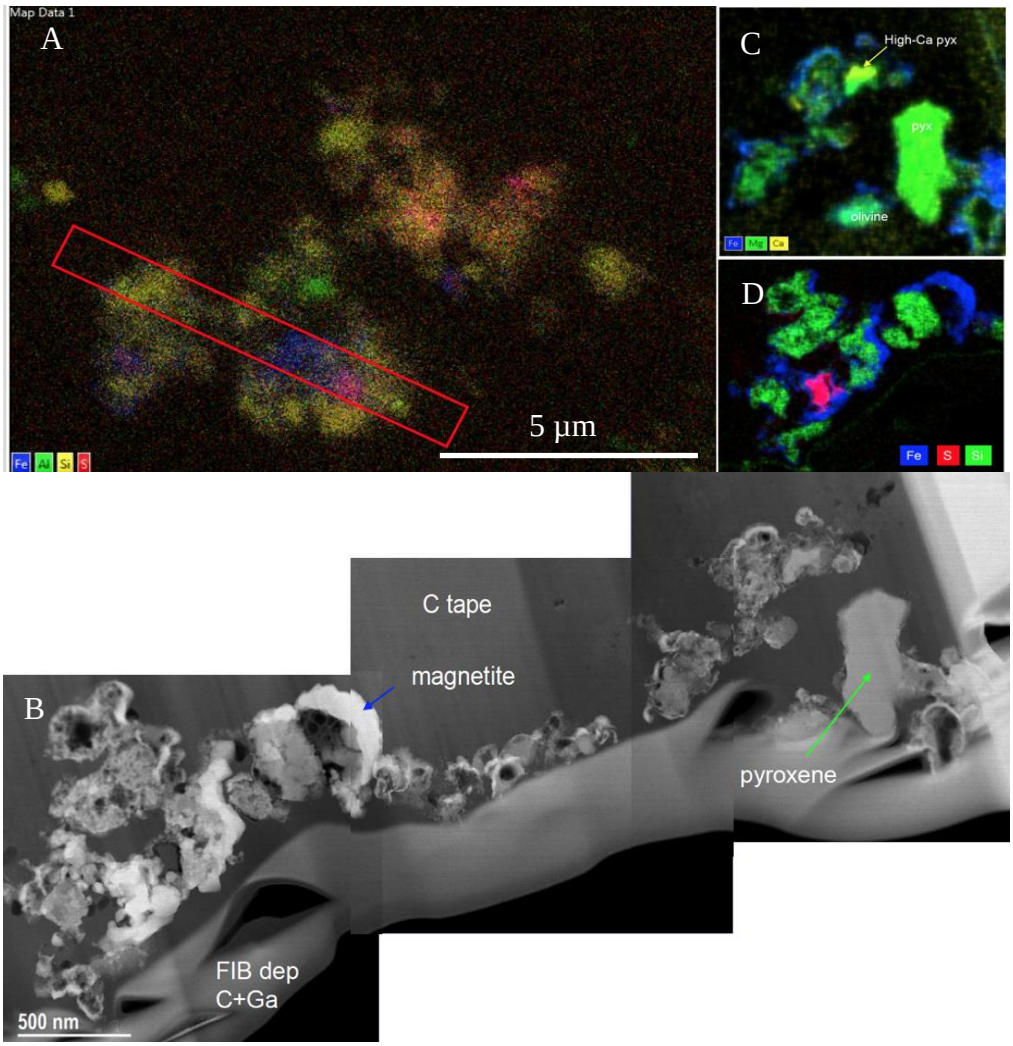

Fig. 9. A) area of particle I removed by FIB; B) overall image of the FIB section; C) Fe, Mg, Ca element map of top right of B; D) Fe, S, Si element map of bottom left of B.

Particle J is a ~5µm hollow sphere of magnetite, sulfide (Ni pyrrhotite), olivine, and pyroxene, which was likely melted during atmospheric entry (Fig. 10). Minor phases rich in Ca (Ca-olivine) and Al (spinel) are present between the larger grains. EELS confirm that the iron-oxide phase is magnetite and that the olivine and iron-sulfide contain no Fe^{3+}. Ni is present only in the pyrrhotite.

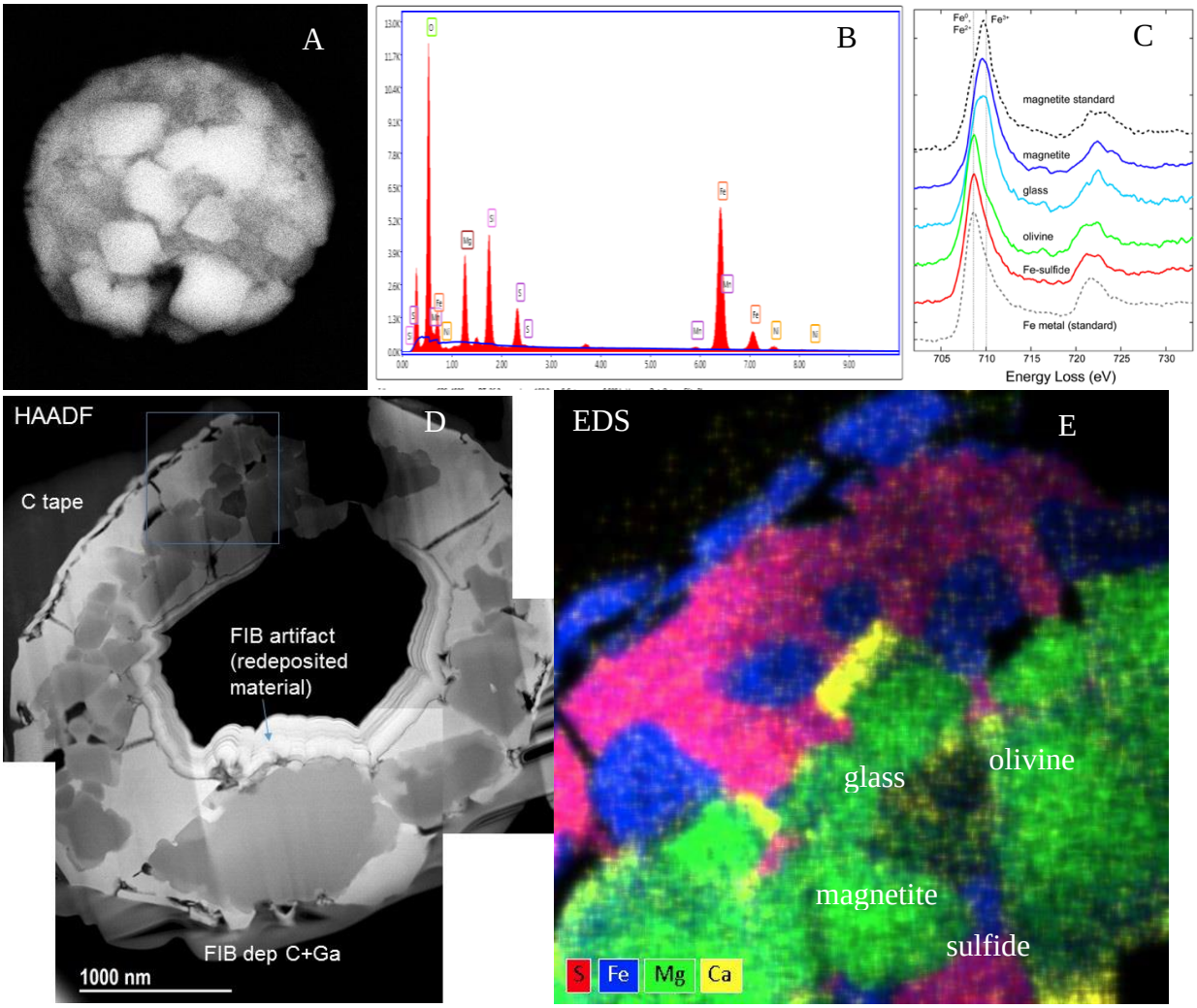

Fig. 10. ET particle J A) SEM image; B) EDAX element analyses; C) EELS spectra: D) HAADF image; and E) EDS map of box area shown in the HAADF image.

One of the more unusual ET candidates is shown in Fig. 11. This particle is irregularly shaped and quite large, 50µm in diameter. It is predominantly carbonaceous with N, O, S and minor amounts of Al, Si, Mg (Fig. 11A). The FIB slices show pores that are near or surrounded by Fe and Ni rich material (Fig. 11B). The Fe is generally associated with P, O and Cr, while Ni is found with S, O and in some places Ca-sulfate and several at% K. Ni-sulfides and Fe-phosphides (or their hydrated/oxidized counterparts) are not common in IDPs, micrometeorites or meteorites. Flynn et al. (2019) found P associated with S in a cluster particle and Fe sulfides with varying amount of Ni in GEMS-rich IDPs (Flynn et al., 2016). Only one Ni sulfide has been seen in a micrometeorite (> 5000 MMs examined, Taylor personal communication) and Belyanin et al. (2018) reported Ni-phosphides in the (also enigmatic) HypatiaStone.

NanoSIMS measurements showed normal H but slightly elevated $^{15}N/^{14}N$ isotope ratios. The average $\delta^{15}N/^{14}N$ of four measurements of three microtomed slices was 47±7 ‰ (Fig. 11C, D). The N isotopes are homogeneous over the particle slices and although the values are not extremely high, they overlap those seen for bulk insoluble organic matter from some meteorites (e.g. CIs have $\delta^{15}N$ ~+30 ‰; Alexander et al., 2007). We are unaware of any terrestrial source of carbonaceous material with such a N-isotope signature and thus think that the enhanced ^{15}N

contents favor an extraterrestrial origin. The particle has no GEMS-like grains but appears to contain enstatite 'whiskers', a feature associated with primitive IDPs (Bradley et al., 1983).

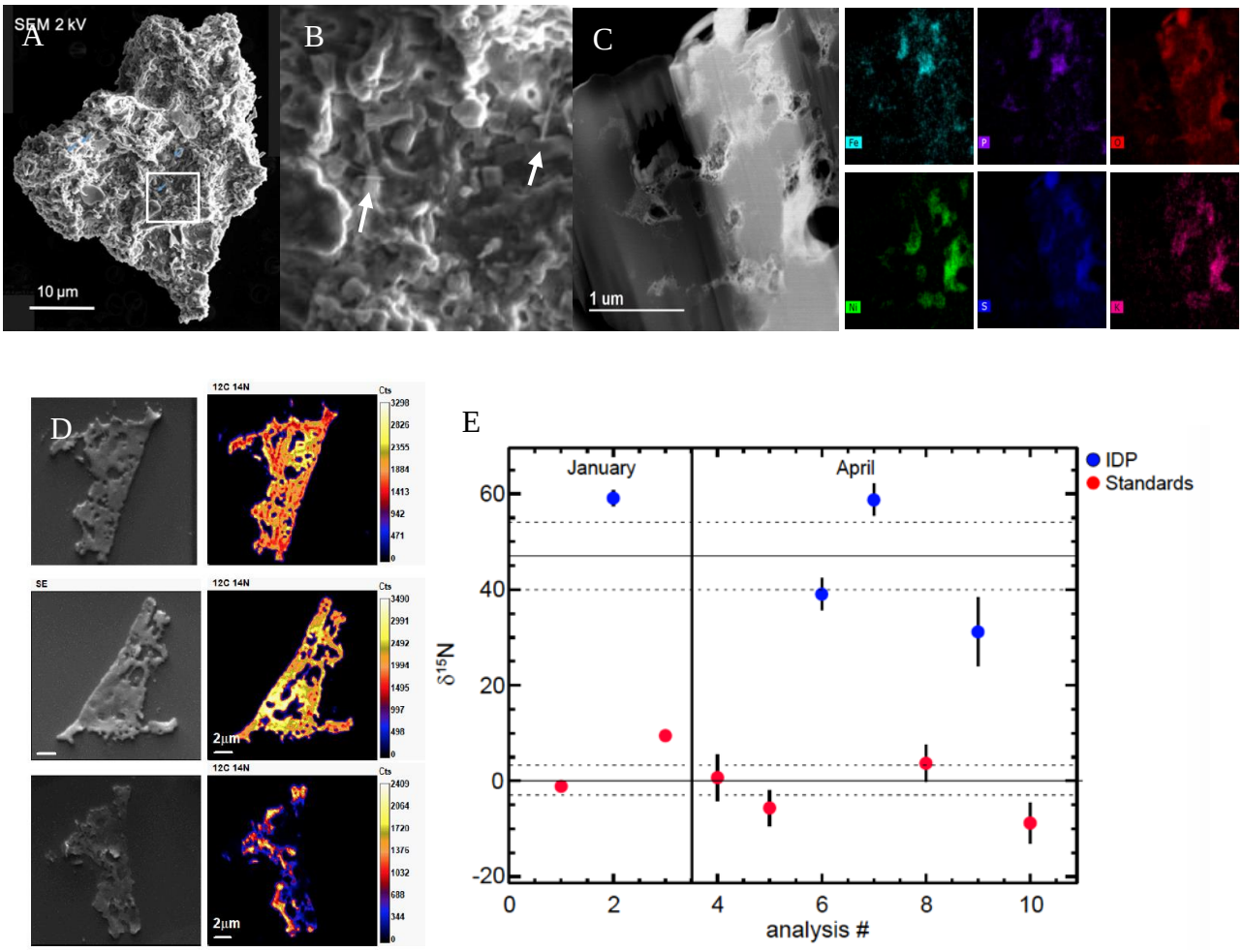

Fig. 11. Carbonaceous ET candidate. A) SEM image of particle; B) magnified section, box in A, showing two enstatite whiskers (arrows); C) STEM of FIB section and element maps; D) microtome sections and corresponding N isotopic maps; E) N isotopic composition of the four microtome sections analyzed.

Helium-3 Measurements

^{3}He above blank levels was detected in 178 of the 180 filter subsamples with amounts ranging from ~2 to ~640 × 10^{-15} cc STP. The average ^{3}He abundance for all 180 cm^2 filter subsamples was 69 x10^{-15} cc/cm^2/month with a median value of 19 x10^{-15} cc/cm^2/month. For stratospheric IDPs the median value is 1x10^{-5} cc ^{3}He/g although the span in ^{3}He concentration is almost a factor of 100 (Pepin et al., 1999).

Using the median values, we estimate the mass of ET material on each subsample at about 2 ng/cm^2/month, equivalent to a 5 µm spherical particle /cm^2/month with typical IDP density (1g cm^{-3} Flynn and Sutton, 1991). This broadly agrees with the original estimate of 1 – 3 IDPs larger than 5 µm/cm^2/month for the South Pole air samples based on measured stratospheric IDP concentrations (Brownlee et al., 1977, Zolensky and Mackinnon 1985).

Temporal variations in ^{3}He concentrations across the ~ 2 year of measurements spanned by the 13 filters are shown in Figure 12. Here we plot the average ^{3}He concentration of the

subsamples, normalized by exposure time, versus the month and year they were collected. We see that the austral spring has elevated ^{3}He deposition relative to other seasons. SPA-1 (30 Nov. 2016) had the highest concentration (1.6×10^{-12}cc STP), followed by SPA-17 (16 Oct. to 7 Nov. 2018) and SPA-35 (22 Oct. to 4 Nov. 2019). The value for SPA-1 is not as certain as those for SPA-17 and 35 because the filter was only exposed for five hours producing a large multiplying factor when normalized. Also, only three subsamples were analyzed. Never the less we think this filter likely has high ET levels because we found an 8µm IDP on the one, 1cm^2 piece of SPA-1 examined by SEM (Fig. 7A) and, furthermore, because the only other filter exposed for a short period of time (SPA-45) had no ^{3}He.

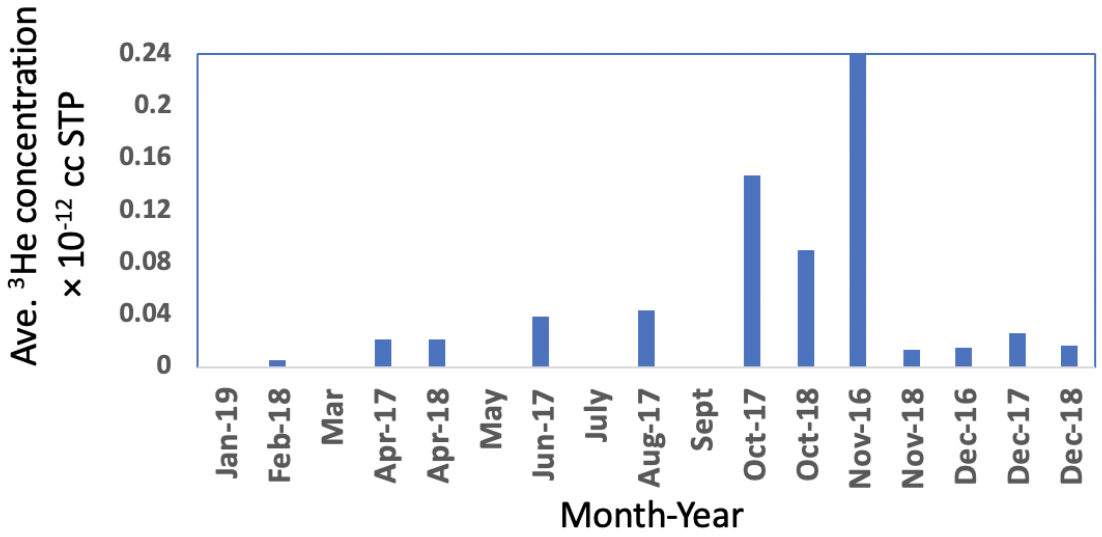

Fig. 12. Average ^{3}He concentrations plotted per month for two years of collection. Concentrations were normalized by filter exposure time. The ^{3}He value for SPA-1 (Nov 2016), lies well above the range plotted at 1.6×10^{-12}cc STP.

To check if the air flow was evenly distributed across the filter, we compared two, 1-cm^2 filter subsamples cut from the edges and two, 1-cm^2 filter subsamples cut from the center of six filters. We found a 4-fold increase in ^{3}He concentration in the center subsamples (Table 2). The average ^{3}He concentration of the two center cm^2 filter pieces is $0.097 \pm 0.17 \times 10^{-12}$cc STP whereas that for the two edge samples of the same filters is $0.023 \pm 0.023 \times 10^{-12}$cc STP. Although there is a large variation in the center subsample values, these values are larger than the edge sample in all cases but one (SPA-13).

IDPs are small and should be entrained in the airflow. Nevertheless, to determine whether ET materials adhered to the intake pipes, we wiped down the inside surfaces of each pipe section with a glass filter and analyzed each for ^{3}He (Fig. 13). The data show that above background concentrations of ^{3}He were found on four of the pipe sections (designated in red) ranging from 0.015 to 0.075×10^{-12}cc STP. As each filter cleaned ~6.2×10^{3} cm^2 of pipe area that was exposed for roughly 25 months, the ET concentrations of the above background filters turn out to be four orders of magnitude smaller than the concentrations on each 1-cm^2 filter subsample. We therefore conclude that insignificant amounts of ET materials are adhering to the pipes.

Table 2. The ^{3}He values ($\times 10^{-12}$cc STP) for two center and edge, 1cm^2 samples taken from of six filters.

Filter #	center	edge
SPA-4	0.0154	0.0123
	0.0225	0.0128
SPA-8	0.0172	0.0077
	0.0227	0.0073
SPA-10	0.0945	0.0114
	0.0800	0.0114
SPA-13	0.0271	0.0468
	0.0342	0.0111
SPA-17	0.0814	0.0420
	0.6372	0.0829
SPA-22	0.1284	0.0161
	0.0024	0.0160
Ave	**0.0969**	**0.0231**
Std	**0.175**	**0.023**

Fig. 13. Schematic of intake pipe sections. Only sections numbered in red had ^{3}He values higher than background.

Discussion

The number of ET particles found on the filter pieces examined is about a third of the number we expected based on the stratospheric concentrations and our air-intake rate (one IDP larger than 5 μm per cm^2 per month of exposure). Although we found smaller and fewer IDPs than we expected, ^{3}He measurements on 180 individual 1-cm^2 pieces of filter indicate an average ET-mass equivalent to one 5-μm IDP per cm^2, comparable to the expected value. Given this agreement in expected mass, the smaller sizes and number of ET particles suggest disaggregation of the IDPs into small pieces that are not easily identified as ET particles on the filters. We do not think that turbulent air-flow systematically disaggregated the IDPs as thin and delicate salt rods survive unbroken (Fig. 5D). Rather, we postulate that exposure to submicron sulfuric acid droplets is the primary cause of IDP disaggregation.

To support this interpretation, we note that some particles on the filters show evidence of having been dissolved. For example, Fig. 14A and B show holes in stainless steel and aluminum particles at the location of the filter pores. We also observe that the majority of small FeNiS beads come from the C sticky mats, initially used to sample particles from the filters. These mats pull material out of the pores where some of the small FeNiS beads were found. Lastly, we found vesicular S-rich material in the interstices of the weather balloon talc particles (Fig. 14C). The S must come from aerosols interacting with the talc either in the atmosphere or while on the filter, as the talc particles contain no S. It is also possible that the IDPs are altered by aerosol droplets in the stratosphere and during transit through the atmosphere to the ground (20 – 70 days for 10-μm particles, depending on their densities).

The South Pole's inaccessibility increases the duration of sulfuric acid exposure relative to other dry IDP collections, for example those describe by Ishii et al. (2018) and Messenger et al. (2015). During the eight-month winter season, the filters cannot be retrieved or analyzed, and return transit of the filters takes several weeks after the station reopens. This lag prolongs the

contact time between the sulfuric-acid aerosols and the IDPs significantly beyond their two-week average residency on the filters during collection. Indeed, we found liquid sulfuric acid in the filter pores two years after collection.

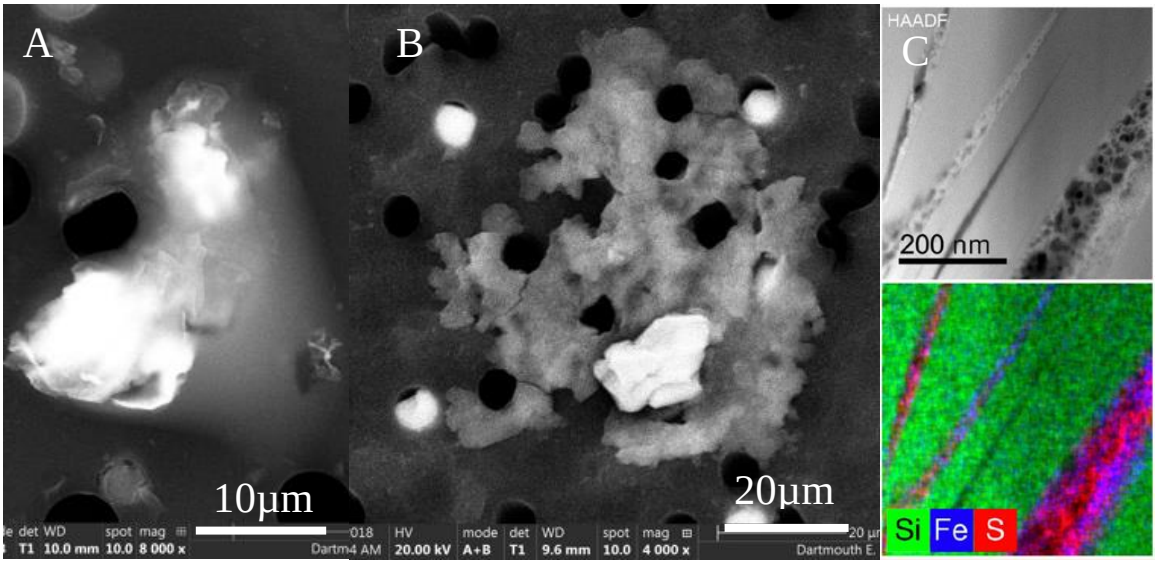

Fig. 14. A) backscatter electron image of a stainless-steel particle in a S-rich droplet; B) Al grain and C) STEM HAADF and EDS of vesicular S-rich material in talc.

Conclusion

We built a collector to obtain 300 – 900 IDPs per month, with the hope of collecting primitive CP- IDPs , cluster particles >30 µm and ultra-carbonaceous MMs. Our sampling strategy used long-duration, continuous dry filtering of surface air in place of short-duration, high-speed impact collection on flags flown in the stratosphere and potentially could sample specific meteor streams and measure seasonal variations in IDP flux. We filtered ~ 10^7 m^3 of clean Antarctic air using 20-cm-dia, 3-µm filter couple with a suction blower of modest power consumption (5 – 6 kW). The high air flow rate through the filter, ~400,000m^3 per month, also delivered myriads of submicron aerosols.

We identified 19 extraterrestrial particles on the 66 cm^2 of filter examined, this area represents ~ 0.5% of all the filter surfaces exposed to the air at South Pole. The 19 ET particles are about a third of what we expected based on stratospheric counts. Of the 19 ET particles, four were CP-IDPs, seven were FeNiS beads, two were FeNi grains and six were chondritic material with FeNiS components. Most were <10µm in diameter and none were cluster particles. We analyzed the ET and ET-candidate particles by a complementary suite of micro-analytical techniques, SEM, STEM, NanoSIMS and EELS. One carbon rich ET candidate particle has a small N isotopic anomaly suggesting it is extraterrestrial. The ^{3}He analyses of 180, 1 cm^2 filter subsamples show the presence of ET matter on 178 of these and that the ET flux appears to vary seasonally. Other bulk measurements, e.g. organics, may also yield interesting results.

As the most primitive ET materials known, IDPs are of great scientific interest. Suctioning them from the air at the surface of the Earth would avoid exposing them to silicone oil, solvents, or water and could potentially collect high numbers of IDPs. Such a continuous record of their arrival is key to assessing any seasonal variations in their flux, determining their background composition, and allowing for timed collections to target meteor streams.

Although there are many advantages in collecting IDPs from the clean air sector at South Pole, these were not fully realized in our project. The large number of Al particles from our intake pipe precluded our finding enough ET particles to characterize the composition of the sporadic micrometeorite flux and its variation. Also, we think that dissolution and disaggregation of IDPs by sulfuric acid aerosols is occurring either during transport to the ground or while sitting on the filter or both.

Future collections could eliminate the Al contamination by using a short, polished intake pipe mounted on the top of a two-story building. The height of the building would obviate a long intake pipe while avoiding snow ingestion. Smaller filter diameters would allow for automated search techniques but would filter less air and collect fewer ET particles. If disaggregation of IDPs is occurring on the filters, the effects of aerosols might be mitigated by dusting the filters with snow during exposure. The snow would protect IDPs from most of the direct aerosol impact (as silicone oil does in the stratosphere) and could be subsequently sublimated. If IDPs are being altered significantly during transport through the atmosphere, exposure to sulfuric-acid aerosols may be a characteristic common to all terrestrial dry-filter collections, as the presence of aerosols is not unique to South Pole.

Acknowledgements

We thank Dr. Jeff Grossman, NASA's Emerging Worlds program manager, for funding this project and for added support provided by Dr. Scott Borg NSF's Antarctic Program manager. We thank our research associates Adam West (2017), Ta-Lee Shue (2018) and Sheryl Seagraves (2019) who conscientiously monitored the operation of the collector and changed out the filters. Many people at South Pole helped to make this project a reality but a special thanks to Leah Street, our NSF science support coordinator and to Dan McCreight, our NSF logistics coordinator. Lastly, we thank our students Amanda Pinson and Summer Christenson from Dartmouth College and David Bour, a NRL SEAP student intern.

References

Alesbrook L. S., Wozniakiewicz P. J., Jones A. E., Price M. C., Ishii H. A., Bradley J. P., and Brough N. 2017. Atmospheric collection of extraterrestrial dust at the Halley VI Research Station, Antarctica, *LPS XLVIII*, abstract #1805.

Alexander C.M.O'D, M. Fogel, H. Yabuta and G.D. Cody (2007) The origin and evolution of chondrites recorded in the elemental and isotopic compositions of their macromolecular organic matter, *Geochimica et Cosmochimica Acta*, 71, 4380-4403.

Belyanin G.A., J. D. Kramers, M. A. G. Andreoli, F. Greco, A. Gucsik, T. V. Makhubela, W. J. Przybylowicz, and M. Wiedenbeck (2018) Petrography of the carbonaceous, diamond-bearing stone ''Hypatia" from southwest Egypt: A contribution to the debate on its origin, *Geochimica et Cosmochimica Acta, 223*, 462–492.

Bodhain B.A., J. J. Deluisi and J. M. Harris (1986) Aerosol measurements at the South Pole, *Tellus*, 33B, 223 – 235.

Bodhain B. A. and M. E. Murphy (1980) Calibration of an automated condensation nuclei counter at South Pole, *Journal of Aerosol Science, 11*, 305-312.

Bradley J.P., D.E. Brownlee, and D.R. Veblen (1983) Pyroxene whiskers and platelets in interplanetary dust: Evidence of vapour phase growth, *Nature*, 301, 473-477.

Bradley J. P. (1994) Chemically anomalous, pre-accretionally irradiated grains in interplanetary dust from comets, *Science*, 265, 925-929.

Brownlee D.E., G.V. Ferry and D Tomandl (1976) Stratospheric Aluminum Oxide, *Science*, 191, 1270-1271.

Brownlee D.E., D.A Tomandl and E. Olszewski (1977) Interplanetary dust: A new source of extraterrestrial material for laboratory studies. *Proc. Lunar Sci. Conf. 8th*, pp 149 – 160.

Busemann H., A.N. Nguyen, G.D. Cody, P. Hoppe, A.L. D. Kilcoyne, R.M. Stroud, T.J. Zega and L.R. Nittler (2009) Ultra-primitive interplanetary dust particles from the comet 26P/Grigg-Skjellerup dust stream collection, EPSL 288, 44–57.

Cosmic Dust Sample catalogs, Vol. 1 (flag W7017), 2 (flag W7029), 7 (flag U2022), 9 (flag U2034), 10 (flag W7074) https://curator.jsc.nasa.gov/dust/catalogs/.

Dartois, E., Engrand, C., Brunetto, R., Duprat, J., Pino, T., Quirico, E., Remusat, L., Bardin, N., Briani, G., Mostefaoui, S., Morinaud, G., Crane, B., Szwec, N., Delauche, L., Jamme, F., Sandt, Ch., Dumas, P. (2013) UltraCarbonaceous Antarctic micrometeorites, probing the Solar System beyond the nitrogen snow-line, *Icarus* 224, 243-252.

Dobrica E., C. Engrand, J. Duprat and M. Gounelle, H. Leroux, E. Quirico and J.-N. Rouzaud (2009) Connection between micrometeorites and Wild 2 particles: From Antarctic snow to cometary ices, *Meteoritics and Planetary Science*, 44, 1643-1661.

Duprat J., E. Dobrica, C. Engrand, J. Aleon, Y. Marrocchi, S. Mostefaoui, A. Meibom, H. Leroux, J-N. Rouzaud, M. Gounelle and F. Robert (2010) Extreme deuterium excesses in ultracarbonaceous micrometeorites from central Antarctic snow, *Science*, 328, 742-745.

Farley K.A., S. Taylor, J. Treffkorn (in prep) Flux of Extraterrestrial Helium to South Pole Air Filters.

Flynn G. J., S. Wirick and P. Northrup (2019) P Speciation in Large, Cluster Interplanetary Dust Particles, 50th Lunar and Planetary Science Conference, held 18-22 March, 2019 at The Woodlands, Texas. LPI Contribution No. 2132, id.1403.

Flynn G. J., L.P. Keller, S. Wirick, W. Hu, L. Li, H. Yan, X Huang, E. Nazaretski; K. Lauer, and Y.S. Chu (2016) High-Nickel Iron-Sulfides in Anhydrous, GEMS-Rich IDPs, 79th Annual Meeting of the Meteoritical Society, held 7-12 August, 2016 in Berlin, Germany. LPI Contribution No. 1921, id.6205.

Flynn G. J., & S. R. Sutton (1991) in: Cosmic dust particle densities - Evidence for two populations of stony micrometeorites, Lunar and Planetary Science Conference, 21st, Proceedings Lunar and Planetary Institute, Houston, TX, p. 541.

Hogan A. W., S. Barnard and J. Bortiniak (1979) Physical properties of the aerosol at the South Pole, *Geophysical Research Letters*, 6, 845-848.

Ishii H. A., P. J. Wozniakiewicz, J. P. Bradley, K. A. Farley and M. Martinsen (2017) Extraterrestrial dust collection at Mauna Loa observatory, Hawai'i, *LPS XLVII*, Abstract #1141.

Ishii, H.A., Bradley, J.P., Dai, Z.R., Chi, M., Kearsley, A.T., Burchell, M.J., Browning, N.D., Molster, F. (2008) Comparison of Comet 81P/Wild 2 dust with interplanetary dust from comets, *Science* 319, 447–450.

Ito, T. (1985) Study of background aerosols in the Antarctic troposphere, *Journal of Atmospheric Chemistry* 3: 69-91.

Mellor, M. (1965) Blowing Snow. Cold Regions Science and Engineering, Part III, Section A3c. Cold Regions Research and Engineering Laboratory, Hanover, NH.

Messenger S., Nakamura-Messenger K., Keller L.P., and Clemett S.J. (2015) 'Pristine stratospheric collection of interplanetary dust on an oil-free polyurethane foam substrate,' *Meteoritics and Planetary Science*, 50: 1468-1485.

Messenger S., L.P. Keller, F.J. Stadermann, R.M. Walker and E. Zinner (2003) Samples of stars beyond the solar system: silicate grains in interplanetary dust. *Science* 300, 105-108.

Messenger S. (2002) Opportunities for the stratospheric collection of dust from short-period comets, *Meteoritics and Planetary Science*, 37: 1491–1505.

Messenger S. (2000) Identification of molecular-cloud material in interplanetary Dust Particles, *Nature* 404: 968-971.

Nittler L.R., C. M.O'D Alexander, J. Davidson, M.E.I. Riebe, R.M. Stroud and J. Wang (2018) High abundances of presolar grains and ^{15}N-rich organic matter in CO3.0 chondrite Dominion Range 08006, *Geochimica et Cosmochimica Acta*, 226, 107-131.

Noguchi T., N. Ohashi, S. Tsujimoto, T. Mitsunari, J. P. Bradley, T. Nakamura, S. Toh, T. Stephan, N. Iwata, and N. Imae (2015) Cometary dust in Antarctic snow and ice: Past and present chondritic porous micrometeorites preserved on the Earth's surface, *EPSL*, 410, 1-11.

Patterson D. B. and K.A. Farley (1998), Extraterrestrial ^{3}He in seafloor sediments: evidence for correlated 100 kyr periodicity in the accretion rate of interplanetary dust, orbital parameters, and Quaternary climate - Orbital inclination, not eccentricity, *Geochimica et Cosmochimica Acta*, 62: 3669–3682.

Pepin R.O., R. L. Palma and D. J. Schlutter (2000) Noble gases in interplanetary dust particles, I: The excess helium-3 problem and estimates of the relative fluxes of solar wind and solar energetic particles in interplanetary space, *Meteoritics and Planetary Science*, 35: 495-504.

Sheridan P., E. Andrews, L. Schmeisser, B. Vasel, J Ogren (2016) Aerosol Measurements at South Pole: Climatology and Impact of Local Contamination, *Aerosol and Air Quanlity Research*, 16: 855-872.

Taylor S., S. Messenger and L. Folco (2016a) Cosmic Dust: finding a needle in a haystack, *Elements*, 12: 171-176.

Taylor S., J. H. Lever, C. M. O'D. Alexander, D.E. Brownlee, S. Messenger, L. R. Nittler, R. M. Stroud, P. Wozniakiewicz, S. Clemett (2016b) Sampling interplanetary dust particles from Antarctic air, 80th Meteoritical Society meeting, Berlin, Germany.

Thomas K. L, G. E. Blanford, L. P. Keller, W. Klock and D. S. McKay (1993) Carbon abundance and silicate mineralogy of anhydrous interplanetary dust particles, *Geochimica et Cosmochimica Acta*, 57: 1551-1566.

Witkowski R.E (1988) A search for the cosmic dust increment to aerosol particles at the geographic South Pole, PhD thesis University of Pittsburgh.

Wozniakiewicz P.J. and 13 others (2014) Initial results from the Kwajalein micrometeorite collections, *LPSC*, pdf 1832.

Zolensky, M.E. and I.D.R. Mackinnon (1985) Accurate stratospheric particle size distribution from a flat plate collection surface. *J. Geophysical Research*, Vol. 90, No. D3, 5801 –5808.

	SPA Filter #	Date Filter Installed	# days Exp	# Day not from CAS	CAS violations	Vol. of air filtered (m3)	Ave flow velocity (m/s)	Ave. outside temp (°C)
Spring	1	30-Nov-2016	**0.25**	**0**		4004	5.9	
	3	30-Nov-2016	**5**	**0**	3	80073	5.9	-28
	4	12-Dec-2017	35	2	4	579512	6.1	-23
Summer	5	9-Jan-2017	25	0	8	441081	6.5	-27
	6	3-Feb-2017	35	6	3	655514	6.9	-39
	7	10-Mar-2017	10	3	0	233433	8.6	-56
	8	20-Mar-2017	28	3	0	539611	7.1	-51
Fall	9	17-Apr-2017	29	11	0	653342	8.3	off scale
	10	16-May-2017	35	2	0	817017	8.6	-47
	11	20-Jun-2017	34	3	0	747530	8.1	off scale
Winter	12	24-Jul-2017	15	0	0	309435	7.6	off scale
	13	8-Aug-2017	14	3	0	288806	7.6	off scale
	14	22-Aug-2017	16	2	0	343093	7.9	-48
	15	7-Sep-2017	39	0	0	762187	7.2	-50
Spring	17	16-Oct-2017	22	0		352322	5.9	-31
	18	7-Nov-2017	23	0		424523	6.8	-27
	21	30-Nov-2017	4	0	9	59716	5.5	-28
	22	4-Dec-2017	14	2	6	254605	6.7	-25
	23	18-Dec-2017	14	1	2	205204	5.4	-21
Summer	24	1-Jan-2018	14	0		201404	5.3	-21
	25	15-Jan-2018	14	0		209004	5.5	-26
	26	29-Jan-2018	14	1	3	220405	5.8	-32
	27	12-Feb-2018	14	0	2	190004	5	-41
	28	26-Feb-2018	14	0		281206	7.4	-45
	29	12-Mar-2018	28	2		448409	5.9	-50
Fall	30	9-Apr-2018	38	1	1	794217	7.7	-49
	31	17-May-2018	21	3	2	399008	7	-54
	32	9-Jul-2018	31	3	0	639499	7.6	-54
Winter	33	27-Aug-2018	28	4	0	600413	7.9	off scale
	34	24-Sep-2018	28	0	0	600413	7.9	-49
Spring	35	22-Oct-2018	13	0	0	278763	7.9	-44
	36	4-Nov-2018	9	0		173446	7.1	-41
	37	13-Nov-2018	7	0		123503	6.5	-33
	38	20-Nov-2018	8	1		130288	6	-30
	39	28-Nov-2018	7	0	2	110202	5.8	-28
	40	5-Dec-2018	6	0	5	96088	5.9	-23
	41	11-Dec-2018	7	0	3	104502	5.5	-21
	42	18-Dec-2018	8	0	4	121603	5.6	-19
Summer	43	26-Dec-2018	7	3	1	108302	5.7	-19
	44	2-Jan-2019	6	1		94459	5.8	-26
	45	8-Jan-2019	1	0		14929	5.5	-28

Appendix A. A condensed version of the Dust Collector data sheet. Filter 2 was a scrap filter, used to protect the blower when the latter was turned off. Filters 16, 19 and 20 were not installed. Filters 19 and 20 were shipped back to the laboratory in Hanover, NH. with their Al covers in place to check if shipping generated Al contamination. Covers were not an important source of Al particles.

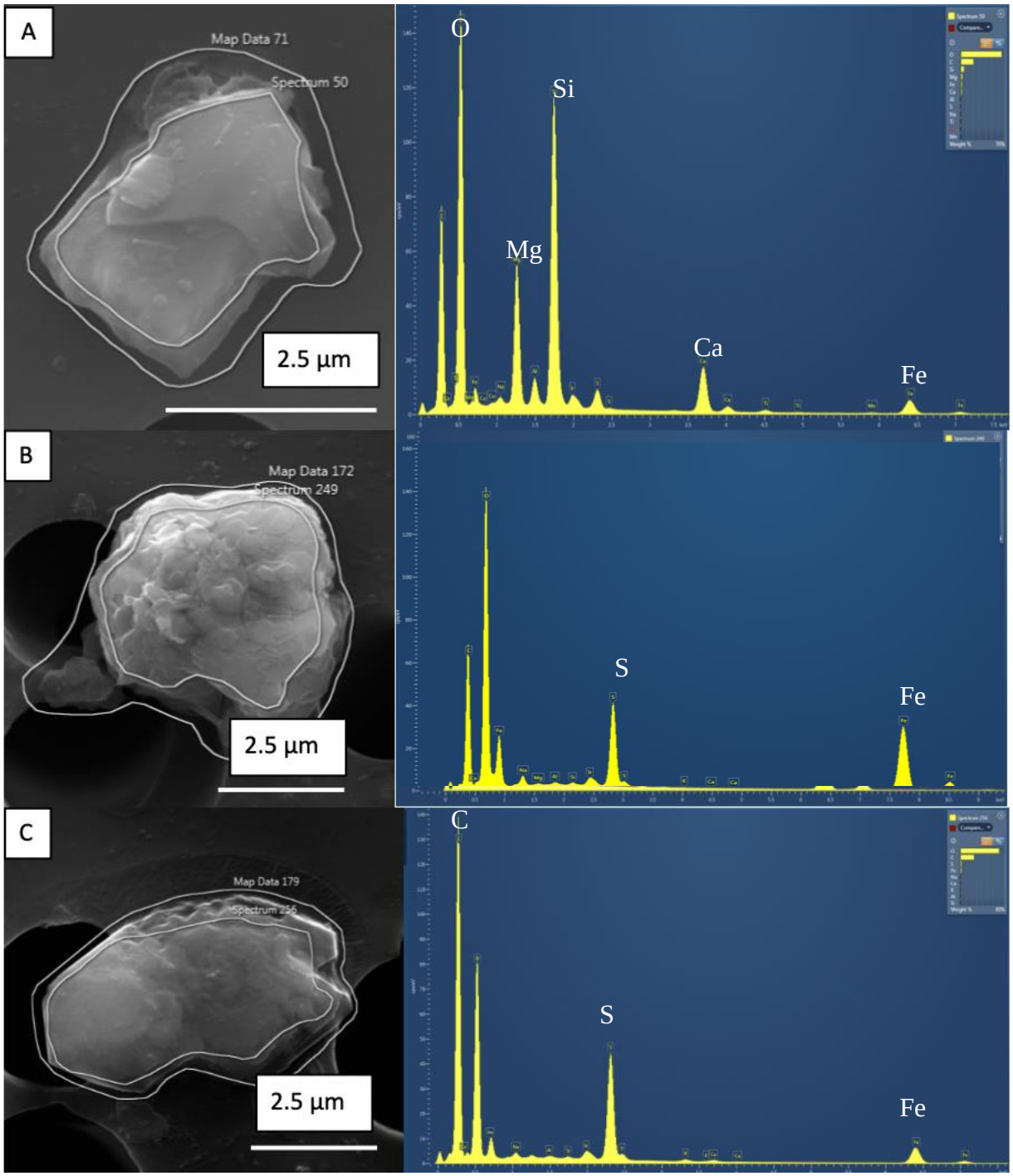

Appendix B. The South Pole air filter have particles of: (A) chondritic glass composition; (B) FeS grains and (C) carbon-rich grains containing sulfides or chondritic components. These types of particles may be classified as cosmic in the Cosmic Dust Catalog.

Vol	flag	# analyzed	# ET	FeNiS beads	Chon +FeNiS	Pyx	Chon glass	CP-IDP	CAT	FeS	Ol	FeNi	CASi
1	W7017A	18	7	1	2			3		1			
	W7017B	16	4		1	1		2					
	W7017C	16	3			1	1						1
	W7017D	14	6		4	1	1						
	W7017E	19	4		1		1	1				1	
	W7017F	16	6	1				2		2		1	
	W7017G	16	3		1		1						1
2	W7029A	19	6	2	1		1	1		1			
	W7029B	18	12		2	1	1	8					
	W7029C	16	6			1	1	3				1	
	W7029D	16	3				2	1					
	W7029E	16	9	1		1	3	1		2	1		
	W7029F	17	5	2	1		1	1					
	W7029G	16	8		3	1		1		1			2
	W7029H	16	6		2		1		2		1		
	W7029I	20	7			1	4	1				1	
	W7029J	15	7			1		3		2			1
SUM		284	102	7	18	9	18	28	2	9	2	4	5
% of Total ET				7	18	9	18	27	2	9	2	4	5
This work		>500	19	7	6	many	many	4	0	>8	1	2	0
% of Total ET				37	32			21				11	

Appendix C. Types of cosmic particles found on flags W7017 and W7029 described in Vol 1 and 2 of the Cosmic Dust Catalog. S.T. classified them based on their EDS spectra and SEM image. Particles were designated CP-IDP if they were multicomponent, fluffy looking particles. We also show the types of ET particles found in this work. No CAT or CAS spherules were found in the South Pole air samples but FeS and chondritic glasses were found. As mentioned in the text we think the enstatite-like particles are talc released from weather balloons.

Chon=Chondritic; CAT=Ca, Al, Ti spheres; CASi= Ca, Al, Si spheres.